LIMNOLOGY
and
OCEANOGRAPHY

ASLO

Limnol. Oceanogr. 60, 2015, 1222–1240

doi: 10.1002/lno.10092

Colored dissolved organic matter dynamics and anthropogenic influences in a major transboundary river and its coastal wetland

Maria Tzortziou,*[1] Christina Zeri,[2] Elias Dimitriou,[5] Yan Ding,[3] Rudolf Jaffé,[3] Emmanouil Anagnostou,[4] Elli Pitta,[3] Angeliki Mentzafou[5]

[1]Department of Earth and Atmospheric Sciences, The City College of New York, City University of New York, New York, New York
[2]Institute of Oceanography, Hellenic Center for Marine Research, Anavyssos, Greece
[3]Southeast Environmental Research Center and Department of Chemistry and Biochemistry, Florida International University, Miami, Florida
[4]Department of Civil and Environmental Engineering, University of Connecticut, Storrs, Connecticut
[5]Institute of Marine Biological Resources and Inland Waters, Hellenic Center for Marine Research, Anavyssos, Greece

Abstract

Most transboundary rivers and their wetlands are subject to considerable anthropogenic pressures associated with multiple and often conflicting uses. In the Eastern Mediterranean such systems are also particularly vulnerable to climate change, posing additional challenges for integrated water resources management. Comprehensive measurements of the optical signature of colored dissolved organic matter (CDOM) were combined with measurements of river discharges and water physicochemical and biogeochemical properties, to assess carbon dynamics, water quality, and anthropogenic influences in a major transboundary system of the Eastern Mediterranean, the Evros (or, Марица or, Meriç) river and its *Ramsar* protected coastal wetland. Measurements were performed over three years, in seasons characterized by different hydrologic conditions and along transects extending more than 70 km from the freshwater end-member to two kilometers offshore in the Aegean Sea. Changes in precipitation, anthropogenic dissolved organic matter (DOM) inputs from the polluted Ergene tributary, and the irregular operation of a dam were key factors driving water quality, salinity regimes, and biogeochemical properties in the Evros delta and coastal waters. Marsh outwelling affected coastal carbon quality, but the influence of wetlands was often masked by anthropogenic DOM contributions. A distinctive five-peak CDOM fluorescence signature was characteristic of upstream anthropogenic inputs and clearly tracked the influence of freshwater discharges on water quality. Monitoring of this CDOM fluorescence footprint could have direct applications to programs focusing on water quality and environmental assessment in this and other transboundary rivers where management of water resources remains largely ineffective.

Over 260 river basins are shared by two or more countries (Wolf et al. 1999). Effective monitoring of water quality and integrated management of fluvial, estuarine, and wetland ecosystem services become particularly challenging in transboundary systems where various authorities, different stakeholders, and international politics often result in conflicting interests and the over-exploitation of some services at the expense of others (De Groot et al. 2006). Upstream interventions often put pressure on downstream ecosystems affecting water quality and ecological dynamics. The *Ramsar* Convention designates more than 2000 wetlands as of international importance, covering more than 200 million hectares worldwide (*Ramsar* List, version 29 January 2014). Almost one third of the *Ramsar* protected wetlands considered in Groombridge (1999) are located in international basins. Despite their enormous ecological and economic value, wetlands around the world continue to be damaged or lost, due to drainage, pollution, nutrient enrichment, and other anthropogenic disturbances (De Groot et al. 2006). Dissolved organic matter (DOM) and its colored component, colored dissolved organic matter (CDOM), are key indicators of water quality, biogeochemical state, and nutrient enrichment (Coble et al. 1998; Fellman et al. 2010; Schaeffer et al. 2013). Due to its influence on water optical properties, CDOM provides a valuable optical tool for tracking DOM sources and monitoring water quality across a range of ecosystems, with potentially powerful applications to assessment of anthropogenic

*Correspondence: mtzortziou@ccny.cuny.edu

influences in transboundary rivers and their highly vulnerable coastal wetlands.

With a strong absorption and fluorescence signal in the visible and ultraviolet (UV) spectral regions, CDOM is one of the major water constituents affecting light attenuation or "water clarity," a critical monitoring parameter in water quality assessment programs, ecological forecasting, and water resource management efforts. Because the optical properties of CDOM depend on its chemical composition, CDOM can be used as a proxy for tracing physical circulation and water-mass history, identifying organic pollution in agricultural and urban catchments, and determining influences of human activities (e.g., land-use change) on stream biogeochemistry and aquatic food-web dynamics (Baker 2002; Fellman et al. 2010). Spectral absorption properties and molar absorptivity have been used as indicators of the molecular size and aromatic content of CDOM (Chin et al. 1994; Del Vecchio and Blough 2004). Simple fluorescence indices and the identification and relative contribution of various fluorescence components in DOM have allowed determining DOM dynamics in relation to biological activity, photochemical processing, microbial consumption, and allochthonous inputs from wastewater, wetlands, forested catchments, and agricultural environments (Baker 2002; Fellman et al. 2010).

Shared by three countries, the Evros river catchment (Bulgarian: *Марица*, Greek: *Έβρος*, Turkish: *Meriç*) is among the most important natural resources in the Balkans, supporting a population of more than 3.6 million people (Kanellopoulos et al. 2009; Skoulikidis 2009). For Bulgaria and Greece, the Evros serves as a water source mainly for agricultural use and hydroelectric power generation. In Turkey, half of the basin is used for irrigational and dry farming. At its mouth, the Evros forms an extended delta of high ecological importance that was designated a Natura 2000 site and is protected under a number of multilateral agreements (UNECE 2011). Despite its economic and ecological importance, the river has been suffering from increasing pollution, fragmentation, flow regulation, and high vulnerability to flooding (Nikolaou et al. 2008; Skoulikidis 2009). Human intervention in the basin increased after the 1950s, with the construction of several dams and reservoirs. Ineffective management of these dams has been suggested to be among the main factors contributing to the observed increase in flood frequency in the downstream part of Evros over the past 13 years (Angelidis et al. 2010). As a transboundary river, the Evros receives industrial waste, agricultural discharge, and urban sewage from the three countries sharing its basin, while discharging high loads of organic and inorganic material to the coastal zone (Kanellopoulos et al. 2009). Freshwater discharge by the Evros river is responsible for more than half of the dissolved organic carbon (DOC) input carried by major Balkan rivers to the Eastern Mediterranean (Skoulikidis 2002), with potentially important implications for coastal photobiogeochemical processes. Yet, there is no information on the composition, optical properties, and distribution of these dissolved organic compounds along the river and coastal waters, or how these are affected by changes in precipitation, wetland contributions, and human activities in this large urban- and agriculturally-influenced watershed.

This study presents the first combined biochemical and optical data for DOM along the continuum of the Evros river, wetlands, estuary, and the coastal zone. Comprehensive measurements of CDOM optical signature and molecular weight (MW) distributions were combined with measurements of precipitation and river discharge, water physicochemical properties, inorganic constituents, DOC and chlorophyll *a* (Chl *a*) concentrations. Measurements were performed over three years, in seasons characterized by largely different river discharges and along transects extending more than 70 km from the freshwater upstream reaches to a marine end-member two kilometers offshore in the Aegean Sea. Our main objective was to examine the complex influences of anthropogenic disturbances (i.e., allochthonous inputs and dam operation) on DOM dynamics in one of the most economically valuable and, simultaneously, particularly vulnerable transboundary rivers of the Eastern Mediterranean and its *Ramsar* protected coastal wetland. Results are particularly relevant to integrated coastal zone management efforts and responses to future pressures, especially as the Eastern Mediterranean is an area that has been identified as a "*hotspot*" in terms of climate change (Giorgi 2006; Lelieveld et al. 2012).

Materials and methods

Site description

Running over 530 km in length, the Evros is the longest river in the Balkan Peninsula and the second largest in terms of water discharge amount in Eastern Europe after the Danube River (Kanellopoulos et al. 2009) (Fig. 1). Its basin is the fifth largest in the Mediterranean, following Nile, Rhone, Ebro, and Po. The Evros total drainage area is approximately 53,000 km^2 of which 66% is in Bulgaria, 27% in Turkey, and 7% in Greece. The river rises on the slopes of Mount Rila in Bulgaria, and receives water from Mount Rodopi and the Antiaimos range via its tributaries Arda and Tundzha. One of its major tributaries, the Ergene (Fig. 1), receives wastewater from many industrial plants in the Turkish Thrace region, including leather tanning and textile industries (Güneş et al. 2008). Forming a natural boundary of 240 km between Greece and Turkey, the Evros flows into the Aegean Sea between the cities of Enez and Alexandroupolis. The average water discharge ranges between 50 $m^3\ s^{-1}$ and 100 $m^3\ s^{-1}$ depending on season (Dimitriou et al. unpubl.) with maximum water discharge in winter (December to April) and minimum in summer (July to September). The climatic and geomorphologic characteristics of the basin lead to run-off

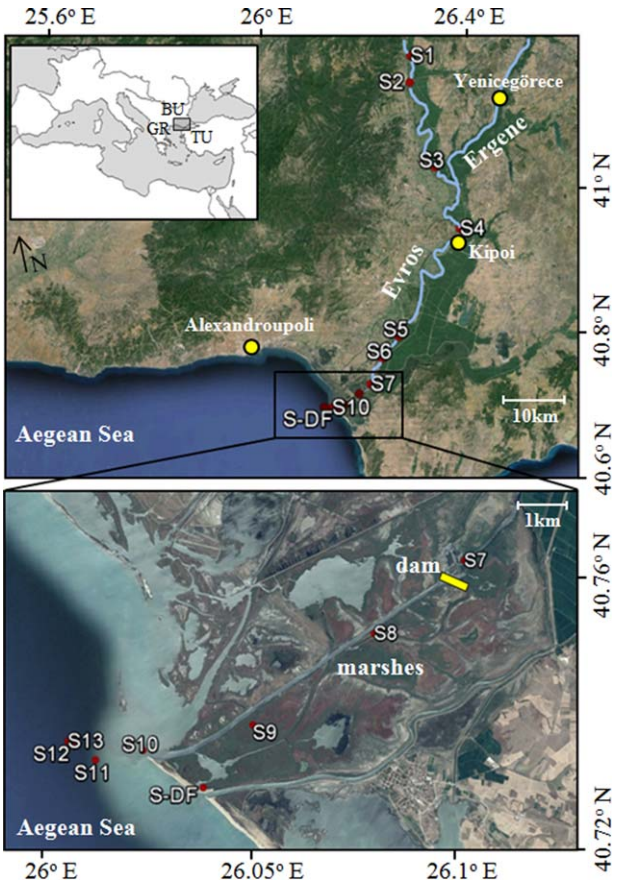

Fig. 1. Map of the 14 sites sampled in the Evros trans-boundary river. (a) Sites extending from the freshwater end-member (S1) to the Aegean coastal waters S13. The location of the Alexandroupoli, Kipoi and Yenicegörece stations where precipitation and river discharge were measured are also shown. (b) Eight sites were sampled in the Evros delta and marshes (S7, S8, S9), river mouth (S10, S-DF), and adjacent coastal waters (S11–S13). The location of the dam is also shown.

conditions characterized by high inter-annual flow variability and favorable conditions for flood events (Maris pers. comm.). Among the most intense over the past 10 years were the floods in February–March 2005 (recurrence interval 1000 years), in January 2006, March 2006 (worst flood in past 50 years), in November 2007, and in February 2010 (UNECE 2011; Dimitriou et al. unpubl.). At its mouth, the Evros forms an extended delta (188 km^2) that has a wide diversity of habitats including freshwater and salt marshes (*Salicornia* sp., *Salsola* sp., and *Phragmites communis*), coastal lakes, lagoons, and sand dunes (*Ramsar* Report Evros Site, 1998). Although in Eastern Mediterranean the tidal range is small, the Evros delta is regularly flooded by sea tides because it is formed lower than the sea level.

Sample collection

To examine spatial dynamics in physicochemical, optical and biogeochemical properties, surface water samples were collected along transects extending from a freshwater end-member approximately 70 km from the shore (site S1; 41.223°N, 26.325°E) to a marine end-member at salinity > 30, two kilometers offshore in the Aegean Sea (site S13; 40.743°N, 26.008°E). Sites S1–S6 are along the Evros freshwater main stem. The area between S3 and S4 is where the Ergene tributary merges with Evros. S7–S10 are brackish sites in the Evros delta. S11–S13 are coastal marine sites in the Aegean sea (Fig. 1).

To examine seasonal and year-to-year variability, measurements were performed during seven samplings that covered different seasons, including spring (wet season), summer (dry season) and early fall (end of dry season), over a three year period (2008–2010) (Table 1). The construction of a small dam downstream of S7 in September 2008 diverted the river flow into a channel to the east of the Evros delta area, in the Turkish side of the basin (Fig. 1b). To examine the influence of the dam on coastal water quality and DOM dynamics, one of our samplings was performed in October 2008. In addition to our regular sampling sites, this sampling included two additional sites: a site in an area in the Evros delta covered by extensive brackish marshes (S8), and a site at the mouth of the channel receiving the diverted flow in the Turkish side of the basin (S-DF). In April 2009, the small dam was already considerably eroded and remained non operational during our samplings in 2009 and 2010.

Hydrological and physicochemical measurements

Discharge measurements (in $m^3\ s^{-1}$, Table 1) were available at the monitoring station Kipoi (D_K), located downstream of S4 in Evros, during three of our samplings (July 2008, April 2009, and September 2009), and at Sta. Yenicegörece on the Ergene river (D_{ERG}), 15 km upstream of the merging with Evros (Fig. 1), during all sampling dates (data available from the Prefecture of Eastern Macedonia—Thrace, the Turkish General Directorate Of State Hydraulic Works, DSI 11th Regional Directorate—Edirne, and the Greek Ministry of Environment, Energy and Climate Change). Daily precipitation values (in mm) were measured consistently at the Orestiada station (National Observatory of Athens, 41.506°N, 26.535°E) and at the Alexandroupoli station (Hellenic National Meteorological Service, WMO16627, 40.850°N, 25.883°E) during 2008–2010 (Fig. 1). The average of the two sites was used as the most representative estimate for the section of the river sampled in this study. From these values, we estimated the total precipitation accumulated over the two months preceding each of our sampling dates (parameter P, in mm; Table 1). This quantity had the best correlation with D_K ($r > 0.7$, $n = 308$, $p < 0.0001$, using all available data in 2008 and 2009) compared to total precipitation accumulated over one-month or three-months prior to each sampling, and can be used as a proxy for water discharge at Kipoi.

Temperature, pH, salinity, and dissolved oxygen (DO), were measured in situ using the portable Hanna HI-9828

Table 1. Salinity (Sal, unitless), ammonium (NH_4^+, in mg L^{-1}) and chloride (Cl^-, in mg L^{-1}) at the sites sampled during our seven samplings. Discharge is reported at the Kipoi station downstream of S4 in Evros (D_K, in m^3 s^{-1}) and at the Yenicegörece station in the Ergene river before the merging with Evros (D_{ERG}, in m^3 s^{-1}). Total precipitation (P, in mm) during the two month period preceding each sampling (average of measurements at Alexandroupoli and Orestiada) is also shown. ("—" indicates no data).

	July 2008			October 2008			April 2009			July 2009			September 2009			April 2010			July 2010		
Station	Sal	NH_4^+	Cl^-	Sal	NH_4^+	Cl^-	Sal	NH_4^+	Cl^-	Sal	NH_4^+	Cl^-	Sal	NH_4^+	Cl^-	Sal	NH_4^+	Cl^-	Sal	NH_4^+	Cl^-
S1	0.0	—	—	0.0	0.01	76.0	0.0	0.02	11.6	0.0	0.08	13.0	0.0	0.01	12.2	—	—	—	—	—	—
S2	0.0	0.03	61.0	0.0	0.01	67.0	0.0	0.02	11.9	0.0	0.07	15.0	0.0	0.02	—	0.0	0.02	16.4	0.0	0.01	20.3
S3	0.0	0.04	57.0	0.0	0.01	68.0	0.0	0.02	13.3	0.0	0.03	—	0.0	0.01	24.8	0.0	0.02	14.8	0.0	0.03	—
S4	0.0	0.49	237.0	0.0	0.49	—	0.0	0.30	30.6	0.0	1.23	—	0.0	0.82	52.9	0.0	0.22	29.2	0.0	0.56	37.8
S5	0.0	1.83	238.0	0.0	1.05	215.0	—	—	—	0.0	0.04	—	0.0	0.56	—	—	—	—	0.0	0.36	35.7
S6	0.9	0.26	—	—	—	—	—	—	—	2.1	—	—	0.0	0.36	51.6	—	—	—	—	—	—
S7	7.0	0.73	—	—	—	—	0.0	—	—	3.1	1.18	—	0.0	0.30	—	0.0	0.16	32.2	0.0	0.1	—
S8	—	—	—	29.7	—	—	—	—	—	—	—	—	—	—	—	0.0	0.15	30.5	—	—	—
S9	14.0	0.93	—	—	—	—	0.0	—	—	2.1	1.34	—	2.1	0.40	—	0.0	0.17	31.9	1.4	—	—
S10	20.0	0.49	—	33.8	0.13	—	2.0	—	—	32.2	0.49	—	6.2	0.13	—	0.9	—	—	2.5	0.17	—
S11	32.0	—	—	37.4	0.01	—	17.0	—	—	33.5	—	—	37.8	0.01	—	—	—	—	4.7	—	—
S12	30.0	—	—	—	—	—	30.0	—	—	—	—	—	—	—	—	—	—	—	—	—	—
S13	35.0	—	—	37.9	—	—	28.0	—	—	35.7	—	—	37.1	—	—	—	—	—	35.0	—	—
S-DF	—	—	—	0.0	0.76	262.0	—	—	—	—	—	—	—	—	—	—	—	—	—	—	—
D_K		17.51			—		113.48				—		31.51				—			—	
D_{ERG}		6.1			8.8		28.0				8.3		15.2				38.8			14.9	
P		25.2			46.6		117.25				37.5		86.25				80.8			103.1	

multiparameter water-quality meter, calibrated before each deployment as required by the international scientific protocol. Water samples of 700 mL and 100 mL were collected for measurements of concentrations of inorganic constituents and chloride, respectively. Samples for inorganic analysis were preserved with 1% $HgCl_2$ (1 mL L^{-1} of sample). Water samples were stored at 4°C and filtered immediately upon arrival at the laboratory. Ammonium (NH_4^+) and chloride (Cl^-) concentrations were measured after filtering water samples through 0.45 μm pore size Whatman cellulose nitrate membrane filters, and concentrations were determined in the soluble fraction by spectrophotometer Pharo 300 Spectroquant (Merck) and ion analyzer 940 Professional IC Vario (Metrohm), respectively.

Chl a and DOC concentrations

Chl *a* concentration was measured fluorometrically using EPA method 445.0 with minor modifications (Arar and Collins 1997). Sample water (150–300 mL) was filtered using 47 mm diameter Whatman GF/F filters. The filters were then folded and placed into 20 mL scintillation vials. Refrigerated samples were extracted (without grinding) in 10 mL 90% acetone/water (v/v) overnight. Fluorescence of the extract was measured on a Turner Designs 10AU fluorometer. The extract was then acidified with two drops 1 N HCl and remeasured. Chl *a* and phaeophytin (data not shown here) were calculated from acidified and nonacidified fluorescence values. The calibration was conducted using pure chlorophyll α (Sigma) as a standard.

Samples for DOC and CDOM analysis were filtered through 0.22 μm Nucleopore filters. Duplicate samples (10 mL) for DOC determinations were stored in precombusted (480°C, 12 h) glass ampoules, acidified with 2.5 mol L^{-1} HCl to pH $\sim$ 2, flame- sealed immediately and kept at 4°C until analysis. DOC concentrations, [DOC], were determined using a Shimadzu (TOC-5000) analyzer and following the methods in Sugimura and Suzuki (1988) and Cauwet (1994). Analytical precision and accuracy were tested against Deep Atlantic Seawater Reference Material provided by the dissolved organic carbon consensus reference materials (DOC-CRM) program (D. A. Hansell, University of Miami). Measured value was 44 ± 3 μmol C L^{-1} ($n = 5$), with a certified value of 45 ± 1 μmol C L^{-1}.

CDOM absorption and fluorescence analysis

Measurements of CDOM absorption were performed using a Cary-4 dual beam spectrophotometer, as described in detail in Tzortziou et al. (2008). CDOM absorption coefficients, a_{CDOM}, were measured in the spectral range from 270 nm to 750 nm (1 nm bandwidth and resolution). Absorption coefficients are reported here at 300 nm, as this is a reference wavelength commonly used in the literature (Table 4 includes estimates at additional wavelengths to facilitate comparison with other studies in Mediterranean rivers and coastal waters). The CDOM absorption spectral slope, S_{CDOM}, was estimated after applying nonlinear exponential regression to absorption values across the full spectral range of the measurements (R^2 values in all cases > 0.99). The average range between duplicate determinations of S_{CDOM} was 0.0001 nm^{-1}. The DOC-specific CDOM absorption coefficients, $a^*_{CDOM}(\lambda) = a_{CDOM}(\lambda)$: [DOC], were also estimated. Both a^*_{CDOM} and S_{CDOM} have been previously proposed as tracers of DOM aromatic content and molecular size, with a^*_{CDOM} typically increasing and S_{CDOM} decreasing with increasing aromaticity and MW (Stewart and Wetzel 1980; Chin et al. 1994).

CDOM fluorescence was measured on a Jobin-Yvon/Spex Fluoromax-3 spectrofluorometer. The fluorescence emission measured by the signal-detector, S_c, was referenced to the signal measured by the reference-detector, R_c, to monitor and correct for fluctuations in the lamp output, according to manufacturer's protocol. Emission and excitation correction-factor files were applied according to manufacturer instructions to correct for the wavelength dependencies of the optical components of each monochromator and the detectors themselves. Three-dimensional fluorescence Excitation-Emission-Matrices, EEMs, were measured at excitation wavelengths from 240 nm to 600 nm (5-nm resolution) and at emission wavelengths from 250 nm to 600 nm (2-nm resolution). Bandwidths were set to 5 nm. Fluorescence spectra were corrected for absorption within the sample (inner-filter effect) according to McKnight et al. (2001). The fluorescence signal of deionized (di) water was measured as a blank and subtracted from the sample spectra to correct for Raman scattering effects. The standard error in the fluorescence measurements was less than 0.5%. The EEMs were analyzed using the traditional "peak picking" technique (Coble et al. 1998; Yamashita and Tanoue 2004; Fellman et al. 2010).

In addition, we estimated two fluorescence indices, the humification index (HIX) and the index of recent autochthonous contribution or biological index (BIX) (Huguet et al. 2009). HIX is the ratio of fluorescence emitted at 435-480 nm to that emitted at 300–345 nm, at excitation 254 nm. High fluorescence HIX values correspond to high fluorescence emission at longer wavelengths, indicating larger contributions from complex molecules and high MW aromatics (Huguet et al. 2009). The BIX has been used in previous studies to determine the presence of the fluorescence marine peak (M) characteristic of autochthonous biological activity (Coble et al. 1998; Huguet et al. 2009). BIX, is calculated at excitation 310 nm, by dividing the fluorescence emitted at 380 nm (maximum of peak M) by the fluorescence emitted at 430 nm (typically, maximum of humic-like fluorescence peak C).

Molecular weight distribution

The MW distribution was determined using size exclusion chromatography–high performance liquid chromatography

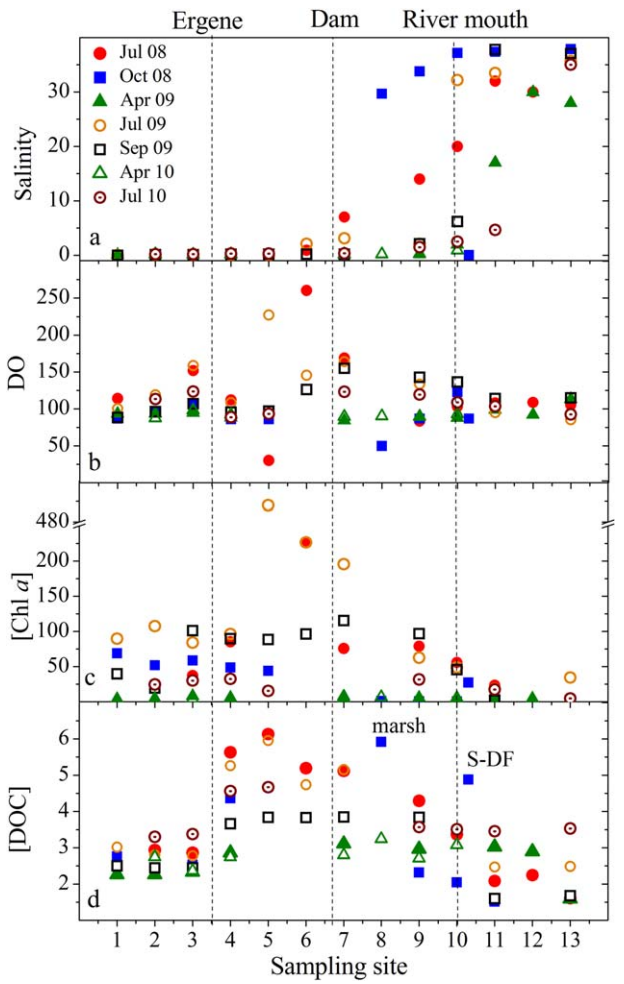

Fig. 2. (a) Salinity (unitless), (b) dissolved oxygen (DO) saturation (in %), (c) chlorophyll *a* concentration ([Chl *a*], in μg L^{-1}), and (d) DOC concentration ([DOC], in mg L^{-1}) along the Evros river for all sample dates. The locations of the merging with Ergene, the river dam, and the Evros river mouth are indicated by dashed lines.

(SEC–HPLC) coupled with a UV-Vis detector as reported in Jaffé et al. (2012). Briefly, the analyses were performed on a Shimadzu (Model LC-10AT) HPLC system fitted with a YMC-Pack Diol-120G size exclusion column (pore size 12 nm, inner diameter 8.0 mm length 500 mm; YMC). An aliquot of 100 μL analyte without pH adjustment was injected into the column directly. The eluent used was 0.05 mol L^{-1} Tris(hydroxymethyl) aminomethane (THAM) adjusted to pH 7.0 with phosphoric acid, eluted at a flow rate of 0.7 mL min^{-1} and measured at 280 nm UV absorption (Scully et al. 2004). The column was calibrated using five poly(styrenesulfonic acid Sodium salt) standards of different and known molecular weights (MW = 1400, 4300, 6800, 13,000 and 32,000 Da, respectively; Sigma Chemical). The void volume ($V_0 = 14.1$ min) and void volume plus inner volume ($V_0 + V_i = 27.5$ min) were determined using Blue Dextran 2000 (Pharmacia, at 628 nm wavelength) and Glycine (Pierce, at 210 nm wavelength), respectively. The weight-average molecular weight (M_w) was calculated as follows: $M_w = \Sigma(AiMi)/\Sigma Ai$, where Ai and Mi are, respectively, the absorbance in arbitrary units and the MW estimated from the calibration curve at elution volume *i*. Determining MW distributions of DOM by SEC with UV detection has been commonly reported in the literature. Following Scully et al. (2004) and Jaffé et al. (2012), M_w is reported here as an index (relative average MW values) to compare the average size of DOM measured under the standard conditions. DOM polydispersity (*d*) was calculated as follows: $d = M_w/M_n$, where M_n (number-average MW) was calculated using the equation $M_n = \Sigma Ai/\Sigma(Ai/Mi)$ (Jaffé et al. 2012). Since salinity strongly affects the SEC distribution, only samples of similar salinity were compared here.

Statistical analysis

Statistical analysis was performed using the SigmaStat/Systat software. The unpaired *t*-test (including the normality test Shapiro–Wilk) was used to calculate the probability that the means of two different samples was statistically significant. The *t* statistic, degrees of freedom (df), and the *p* value are reported. The Pearson Product Moment Correlation was used to measure the strength of the association between pairs of variables. The correlation coefficient, *r*, the number of samples, *n*, and the *p* value are reported.

Results

Hydrologic and physicochemical conditions

Precipitation (P) and river discharge (D_K and D_{ERG}) in the Evros catchment showed large seasonal variability (Table 1). Relatively high precipitation (P > 80 mm during the two month period preceding each sampling) was measured for both our samplings in spring (wet season), while precipitation and discharge were lower in summer (dry season) (Table 1). This is typical for semiarid Mediterranean systems. Based on the long term data series (1970-2010) available at the Alexandroupoli station, the average total monthly precipitation decreases from 55.4 mm, 44.8 mm, and 35.3 mm, in February, March, and April, respectively, to 26.9 mm, 23.7 mm, and 13.7 mm in June, July, and August. An exception was the June–July 2010 period. Total rainfall amounts were 46.4 mm in June 2010 and 45.8 mm in July 2010, more than twice the long-term (1970-2010) monthly average. Total rainfall reached as high as 103 mm during the two months preceding our sampling in July 2010, compared to < 38 mm during the two months preceding our samplings in July 2008 and July 2009 (Table 1).

Changes in precipitation directly affected salinity gradients, resulting in a seasonal transition between freshwater and saline regimes in the Evros delta and coastal waters (Fig. 2a). Superimposed on the influence of precipitation was the influence of the dam on freshwater flow regulation.

Table 2. Salinity (unitless), DOC concentration (mg L^{-1}), S_{CDOM} (nm^{-1}), a_{CDOM} (300) (m^{-1}), and a^*_{CDOM} (300 nm) ($m^2\ g^{-1}$) measured in the freshwater segment of the river upstream (FW u-Ergene) and downstream (FW d–Ergene) of the merging with Ergene, in the Evros marshes, the river delta, and coastal waters (average value, SD in parenthesis, and range of values are shown). Downstream the location of the dam, results are shown for samplings when the dam was operational (October 2008) and when the dam was not operational (all other samplings), and at the site receiving the diverted river flow in October 2008 (S-DF).

	Salinity	DOC	S_{CDOM}	$a_{CDOM}(300)$	$a^*_{CDOM}(300)$
FW u-Ergene	<1	2.75 (0.41)	0.0174 (0.0007)	8.11 (1.30)	3.03 (0.46)
(S1–S3) All transects		2.26–3.71	0.0160–0.0186	5.49–9.88	2.24–3.77
FW d-Ergene	<1	4.53 (1.06)	0.0161 (0.0008)	15.48 (3.46)	3.46 (0.50)
(S4-S6) All transects		2.75–6.13	0.0145–0.0173	10.70–20.13	2.93–4.62
Marshes (S8)	29.7 ($n = 1$)	5.92 ($n = 1$)	0.0168 ($n = 1$)	23.56 ($n = 1$)	3.98 ($n = 1$)
Dam operational (October 08)					
River delta (S7, S9, S10)	3.8 (5.9) 0.0–20.0	3.56 (0.52)	0.0167 (0.0005)	11.68 (2.27)	3.32 (0.53)
Dam non operational		2.71–5.15	0.0157–0.0177	8.69–16.57	2.60–4.06
River delta (S7, S9, S10)	35.5 (2.4) 33.8–37.2	2.09 (0.21)	0.0193 (0.0002)	3.55 (0.31)	1.81 (0.25)
Dam operational (October 08)		1.90–2.31	0.0192–0.0195	3.33–3.77	1.63–1.98
Coastal waters (S11–S13)	29.5 (10.2) 4.7–37.9	2.39 (0.71)	0.0190 (0.0039)	5.80 (3.90)	2.20 (1.06)
Dam non operational		1.59–3.53	0.0165–0.0301	0.85–11.73	0.53–3.78
Coastal waters (S11–S13)	37.4 ($n = 1$)	1.52 ($n = 1$)	0.0210 ($n = 1$)	1.51 ($n = 1$)	1.0 ($n = 1$)
Dam operational (October 08)					
S-DF Dam operational (October 08)	0.05 ($n = 1$)	4.88 ($n = 1$)	0.0157 ($n = 1$)	17.84 ($n = 1$)	3.66 ($n = 1$)

Maximum salinity was measured in the Evros delta following the construction of the dam in October 2008. Salinity reached 29.7 in the marshes (S8) compared to almost zero in April 2010, and 35.5 at the mouth of the delta (S10) compared to an average value of 14 (Fig. 2a). At the marine end-member (S13), salinity varied between 28 and 37.9, with the lowest value in April 2009 and maximum in October 2008.

Dissolved oxygen (DO) variability in the river was mostly biologically rather than physically driven, as indicated by the almost no correlation with water temperature. DO conditions remained close to saturation (99% on average) at our upstream freshwater sites S1–S2, with slightly higher values (by 11%) during summer (Fig. 2b). Highly variable conditions, with DO as low as 30% to as high as 260% (standard deviation (SD) = 44%) were observed downstream of the merging with Ergene during the dry season, with the highest DO (> 160%) coinciding with particularly high Chl *a* concentrations. DO in this segment of the river was lower and considerably less variable during the wet season (90%, SD = 2%). Low variability was observed during both wet and dry seasons in the coastal waters, where DO was close to saturation (102%, SD = 9%) suggesting well oxygenated waters. Undersaturated waters (< 50%) were observed in the Evros marshes during the October 2008 sampling.

Inorganic constituents, Chl *a*, and DOC dynamics

Ammonium (NH_4^+) and chloride (Cl^-) concentrations consistently increased downstream of the merging with Ergene, NH_4^+ by more than an order of magnitude and Cl^- by more than a factor of two (Table 1). In October 2008, NH_4^+ was below detection (< 0.01 mg L^{-1}) in the coastal waters downstream of the river dam and off the Evros main stem, while both NH_4^+ and Cl^- remained at high levels in the coastal waters receiving the diverted freshwater discharge (site S-DF).

Chl *a* was relatively low during spring, with an average concentration of 5.5 μg L^{-1} (SD = 1.4 μg L^{-1}) in the freshwater-brackish segment of the river and 3.5 μg L^{-1} (SD = 1.2 μg L^{-1}) at the marine end-member (Fig. 2c). Considerably higher Chl *a* amounts and variability (67 μg L^{-1} on average, SD = 81.8 μg L^{-1}) were observed during the summer and fall months. Maxima in Chl *a* were often observed downstream of S3, with concentrations exceeding in some cases 200 μg L^{-1}.

DOC concentrations varied both spatially and temporally (1.52–6.13 mg L^{-1}) (Fig. 2d; Table 2). Freshwater DOC showed statistically significant seasonal variability (*t*-test, $t = -3.248$, df = 26, $p = 0.003$) with higher concentrations (4.32 mg L^{-1}, SD = 1.21) during the warm summer months, particularly following high precipitation in July 2010, and lower in spring (2.96 mg L^{-1}, SD = 0.85). In addition to this seasonal variability, DOC showed large spatial gradients

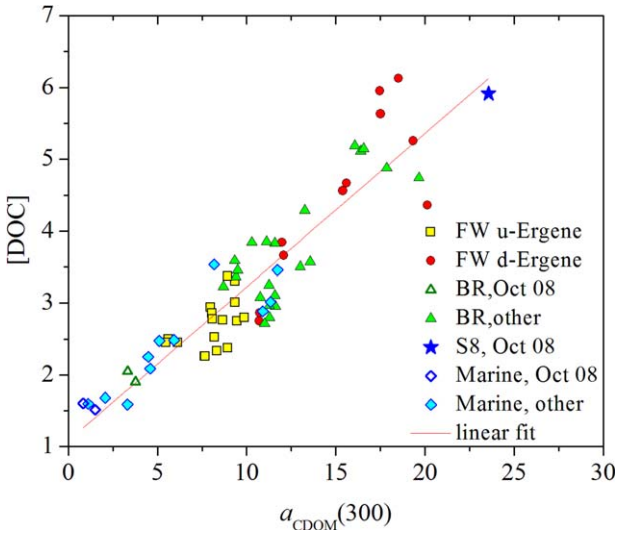

Fig. 3. Relationship between DOC concentration ([DOC], in mg L^{-1}) and CDOM absorption at 300 nm (in m^{-1}), for measurements at: freshwater sites upstream the merging with Ergene (FW u-Ergene), freshwater sites downstream the merging with Ergene (FW d-Ergene), brackish sites during October 2008 (BR, October 08), brackish sites all samplings other than October 2008 (BR, other), Evros marsh (S8) during the October 2008, marine sites for October 2008 (Marine, October 08), and marine sites all samplings other than October 2008 (Marine, other). The linear regression between all measurements of DOC and CDOM absorption is also shown (liner fit; $r = 0.92$, $n = 68$, $p < 0.0001$).

along the river. While [DOC] was relatively low upstream of S3 (2.75 mg L^{-1}, SD = 0.41), a sharp increase by almost a factor of two was consistently observed at S4 with [DOC] remaining elevated (on average 4.53 mg L^{-1}) more than 25 km downstream. Variability in the delta and coastal zone was driven by changes in water discharge, with relatively high [DOC] (> 3.5 mg L^{-1}) extending out to the Aegean Sea under high discharge conditions. Low values (< 2.0 mg L^{-1}) were observed in the coastal waters downstream the dam and off the Evros main-stem in October 2008, while [DOC] was as high as 4.88 mg L^{-1} at the mouth of the channel receiving the diverted freshwater flow (S-DF). A consistent high peak in [DOC] was observed in the marshes (S8), particularly during the October 2008 sampling when the marsh area remained unaffected by upstream freshwater inputs.

DOC was strongly correlated with CDOM absorption ($r = 0.92$, $n = 68$, $p < 0.0001$; Fig. 3). Extrapolation of the linear regression to zero a_{CDOM} (Fig. 3) provides an estimate of the nonabsorbing fraction of DOC. This was 1.08 ± 0.13 mg L^{-1} at 300 nm ($p < 0.0001$), or approximately 33% of DOC on average over all seasons. The absorbing DOC component was on average higher (80%) in the freshwater segment of the river, decreasing to 64% in the brackish estuarine waters and 40% at the marine end-member. Estimates of seasonal trends showed an average decrease in the fraction of absorbing DOC from 70% in spring to 58% in early-mid fall.

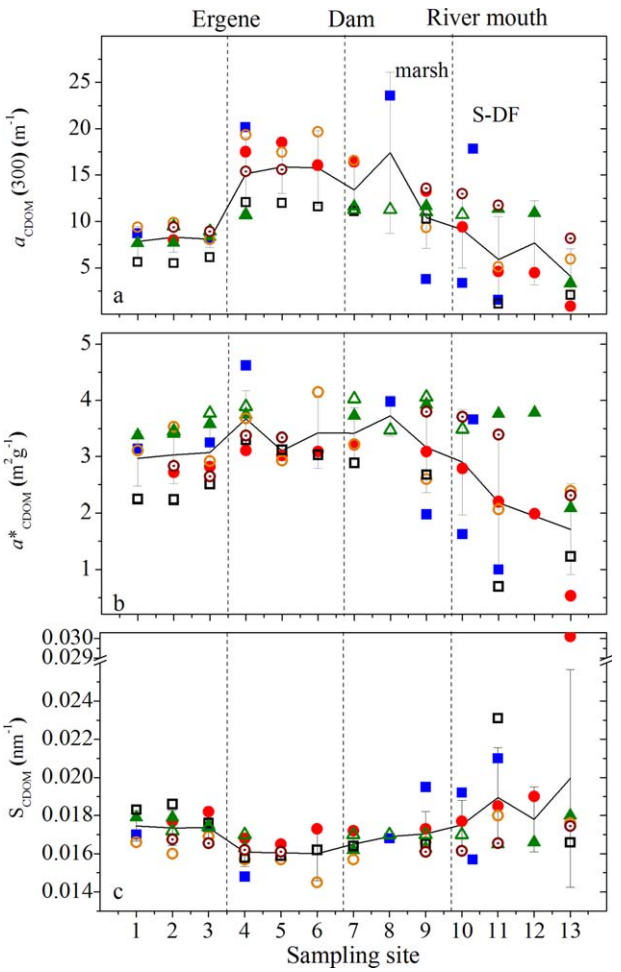

Fig. 4. Change in CDOM absorption properties along Evros for all sample dates. Average values (over all sampling dates, at each site) are shown as solid line, while variability among sampling dates (1 SD) is shown by the error bar. Symbols are same as in Fig. 2.

CDOM absorption characteristics

Although variability in CDOM was driven partly by changes in DOC amounts, observed gradients in both DOC-specific CDOM absorption and spectral slope (quantities strongly inversely correlated, $r = -0.73$, $n = 68$, $p < 0.0001$) reflected parallel changes in DOM composition (Fig. 4; Table 2). Whereas freshwater DOM showed small spatial gradients and no clear seasonal dependence upstream of S3, a steep increase in a_{CDOM} (by a factor of 2) with a parallel increase in a^*_{CDOM} and decrease in S_{CDOM} were observed downstream the merging with Ergene, particularly during the dry season. Absorption remained elevated while S_{CDOM} remained low almost 25 km downstream (Fig. 4). A gradual decrease in a_{CDOM} and a^*_{CDOM} with a simultaneous increase in S_{CDOM} were found in the Evros delta (S7–S10) under dry conditions (i.e., > 40% decrease in a_{CDOM}), while CDOM properties remained almost constant (< 5% decrease in a_{CDOM} and almost no change in S_{CDOM}) during high water discharge.

Table 3. Major peaks (ex/em wavelengths) identified in CDOM fluorescence EEMs, estimated fluorescence humification (HIX) and biological (BIX) indices, and fluorescence peak ratios (average values with SDs shown in parentheses). Results are shown for the freshwater segment upstream (FW u-Ergene) and downstream (FW d-Ergene) of the merging with Ergene, in the Evros marshes (for comparison results are also shown for brackish marshes in the Chesapeake Bay), the Evros river delta when the dam was operational (October 2008) and when it was not operational (all other samplings), and in the coastal waters ("n/o" indicates peak was not observed).

			Marshes		River delta		Coastal waters	
Fluorescence peaks and indices	**FW u-Ergene All transects**	**FW d-Ergene All transects**	**Evros October 08**	**Chesapeake November 08**	**July 08, April 09, July 09, September 09, April 10, July 10**	**October 08 (dam operational)**	**April 09, July 09, September 09, July 10**	**July 08, October 08**
UVC humic-like, A	240/445	250/460	240/445	240/445	250/460	240/445	250/460	(240/445)
UVA humic like, M	310/410	n/o	n/o	n/o	n/o	n/o	n/o	n/o
Tyrosine-like, B	280/(310–330)	n/o	280/305	280/305	n/o	280/305	n/o	280/310
Tryptophan-like, T1	n/o	280/335	n/o	n/o	280/335	n/o	280/335	n/o
Tryptophan-like, T2	n/o	240/350	n/o	n/o	240/350	n/o	240/350	(240/340)
Unknown, P	n/o	300/460	n/o	n/o	300/460	n/o	300/460	n/o
UVC humic-like, C	n/o	360/460	330/440	330/440	360/460	330/440	360/460	n/o
HIX	6.95 (1.55)	6.26 (1.01)	8.08	9.7	6.23 (0.51)	2.94	3.20 (1.01)	0.75 (0.41)
BIX	0.71 (0.06)	0.57 (0.05)	0.64	0.60	0.61 (0.04)	0.8	0.7 (0.05)	0.9 (0.10)
M : A	0.5 (0.05)	n/o	n/o	n/o	n/o	n/o	n/o	n/o
B : A	0.2 (0.09)	n/o	0.15 ($n = 1$)	0.12 ($n = 1$)	n/o	1 ($n = 1$)	n/o	4.7 (2.64)
T1 : A	n/o	0.2 (0.03)	n/o	n/o	0.3 (0.03)	n/o	0.5 (0.1)	n/o
T2 : A	n/o	0.5 (0.2)	n/o	n/o	0.5 (0.1)	n/o	0.9 (0.2)	1.2 (0.61)
P : A	n/o	0.3 (0.1)	n/o	n/o	0.3 (0.1)	n/o	0.3 (0.1)	n/o
C : A	n/o	0.2 (0.1)	0.38 ($n = 1$)	0.45 ($n = 1$)	0.2 (0.1)	n/o	0.2 (0.1)	n/o

Table 4. CDOM properties and DOC amounts in various Mediterranean rivers and coastal waters.

Study Area	Source	DOC (mg L^{-1})	a_{CDOM} (λ) (m^{-1})	S_{CDOM} (nm^{-1})	Peaks
N. Tyrrhenian Sea; Arno River estuary, plume and coastal waters	*Seritti et al. (1998) (Arno River estuary, Salinity: 4.9–10.9)*	3.35–4.82 Average=4.06	a_{CDOM}(280): 16.80-21.60 Average =19.64	0.0166-0.0169 Average= 0.0167	T (280/340–350) C (355/450–460)
	(Arno River coastal, Salinity: 35.2-36)	1.02-1.19 Average=1.10	a_{CDOM}(280): 1.28-2.43 Average = 1.76	0.0114-0.0256 Average= 0.0171	T (280/340–350) C (355/450–460)
	Vignudelli et al. (2004) (Arno River coastal, Salinity<37)	0.84-0.91			B (280/340–350) C (355/440–450)
	Vignudelli et al. (2004) (Arno river, Salinity=9)	3.86			B (280/340–350) C (355/440–450)
Northern Adriatic Sea: Tagliamento, Po, Adige River plumes, and coastal waters	*Berto et al. (2010) (Po prodelta/coastal, Salinity: 34.6±2.3)*	Average = 1.86 ±0.37	a_{CDOM}(280) Average =2.2	Average=0.0207 ±0.0052	
	Babin et al. (2003) (Po, Tagliamento, Adige River plumes)		a_{CDOM}(443): 0.03-0.35	0.0161-0.024 Average= 0.0192	
	Obernosterer and Herndl (2000) (N. Adriatic coastal) Ferrari et al. (1996) (Po di Volano upstream) (Adriatic coastal waters)	0.88-1.81	a_{CDOM}(365) Average=0.124±0.05 a_{CDOM}(350): 17.00 a_{CDOM}(350): 1.00		
Gulf of Lions, Rhone river plume	*Para et al. (2010) (Rhone River, Arles station: freshwater)*	Average=1.63 ±0.45 (TOC)	a_{CDOM}(350) Average = 2.42±1.05	Average= 0.0170±0.001	A (260/430–440) B (275/300–310) T (275/330–350) C (350/430–450) M (300/380–400)
	Babin et al. (2003) (Rhone river plume)		a_{CDOM}(443): 0.01–0.30	0.0114-0.0251 Average=0.0170	
	Ferrari (2000) (Salinity: 34–38) Bricaud et al. (1981) (Golf of Fos–sur-Mer and Etang de Berre, highly contaminated). (Emicort, near discharge of Marseilles drains)	0.65–4.75	a_{CDOM}(355): 0.07–1.71 a_{CDOM}(375): 0.20–1.33 a_{CDOM}(375): 0.16–1.41	0.0110-0.0280 Average=0.0130 Average=0.0120	
Banyuls-sur-Mer, France	*Abboudi et al. (2008) 500 m offshore (Salinity=37.7) Canet Lagoon - Eutrophic (Salinity=7.5)*	1.00 10.7	a_{CDOM}(350) = 0.46 a_{CDOM}(350) = 7.73		
Villefranche Bay	*Bricaud et al. (1981) (coastal area)*		a_{CDOM}(375): 0.15–0.40	Average=0.0140	
Fuirosos catchment, intermittent flow	*Vázquez et al. (2011)*	1.00-6.00	$SUVA_{254}$: 0.10-2.40		A (260/410–430)
	Vázquez et al. (2007)	2.00–4.00 10.00–20.00			B (240/300–310)

TABLE 4. Continued

Study Area	Source	DOC (mg L^{-1})	a_{CDOM} (λ) (m^{-1})	S_{CDOM} (nm^{-1})	Peaks
	(basal discharge) (hydrological transition)				(280/300-310) C (330/410-430)
Evros river, delta, and N.Aegean coastal waters	*This study (freshwater-brackish area, Salinity: 0-37, Average Salinity=2.75)*	1.90-6.13 Average=3.52	a_{CDOM}(280): 4.89-32.94 Average =16.09 a_{CDOM}(350): 1.28-10.19 Average = 4.96 a_{CDOM}(375): 0.79-6.71 a_{CDOM}(443): 0.22-2.47	0.0145-0.0195 Average=0.0170	A (240-250/445-460) M (310/410) B (280/305-330) T1 (280/335) T2 (240/350) P6 (300/460) C (330-360/440-460)
	This study (Evros delta-coastal area, Salinity: 5-38, Average Salinity=30)	1.52-3.53 Average=2.32	a_{CDOM}(280): 1.55-16.34 Average = 7.78 a_{CDOM}(350): 0.19-5.13 Average = 2.28 a_{CDOM}(375): 0.09-3.39 a_{CDOM}(443): 0.01-1.10	0.0165 - 0.0301 Average=0.0191	A (240-250/445-460) B (280/305-310) T1 (280/335) T2 (240/340-350) P6 (300/460) C (330-360/440-460)

Under such conditions, strongly absorbing and low slope CDOM was exported to the coastal Aegean, with $a_{CDOM}(300)$ as high as 11.73 m^{-1} and S_{CDOM} as low as 0.0165 nm^{-1} more than 1.5 km offshore (S12). Under dry conditions (July 2008, July 2009), CDOM in these coastal waters was characterized by considerably lower absorption (4.1 m^{-1}, SD = 3.0), lower a^*_{CDOM} (1.71 m^2 g^{-1}, SD = 0.81) and higher S_{CDOM} (0.0200 nm^{-1}, SD = 0.0057) (Fig. 4).

Dam-induced changes in water flow regimes in October 2008 dramatically affected coastal CDOM quality. Intrusion of saltwater introduced weakly absorbing and high slope marine CDOM ($a_{CDOM}(300) = 3.55$ m^{-1}, $S_{CDOM} = 0.0193$ nm^{-1}) into the Evros delta, while strongly absorbing and low slope CDOM ($a_{CDOM}(300) = 17.84$ m^{-1}, $S_{CDOM} = 0.0157$ nm^{-1}) was found in the coastal waters off the mouth of the channel receiving the diverted freshwater flow (S-DF). Under this flow regime, CDOM in the marshes was characterized by particularly high a_{CDOM}, high a^*_{CDOM} and low S_{CDOM} (23.56 m^{-1}, 3.98 m^2 g^{-1} and 0.0168 nm^{-1}, respectively) (Fig. 4; Table 2).

CDOM fluorescence characteristics

The HIX index, showed a gradual decrease with increasing salinity from 6.95 to 0.75, with the exception of a peak (HIX = 8.08) in the marsh (Table 3). Variability in HIX upstream of S3 was driven by changes in precipitation ($r = 0.82$, $n = 7$, $p = 0.024$), while downstream of S3 HIX was not correlated strongly with precipitation ($r = 0.4$, $n = 7$, $p = 0.37$). In the Evros delta, HIX remained relatively high (6.23, SD = 0.51), but decreased to < 3.0 when the dam was operating (Table 3).

BIX ranged between 0.63 and 0.77 upstream of S3 and was strongly correlated with changes in Chl *a* ($r = 0.86$, $n = 7$, $p = 0.012$). Downstream S3, BIX was statistically significantly lower (0.49-0.65; *t*-test, $t = 4.960$, df = 12, $p < 0.001$), became inversely correlated with Chl *a* ($r = -0.76$, $n = 7$, $p = 0.046$) and positively correlated with total precipitation and discharge from Ergene ($r = 0.84$, $n = 7$, $p = 0.018$). BIX, remained relatively low in the Evros marshes and at coastal sites influenced by the Ergene outflow, while it increased in the river delta and reached 0.9 (SD = 0.1) at the marine end-member during low freshwater influence (Table 3).

Three main peaks were identified in the fluorescence EEMs of freshwater CDOM upstream of S3 (Table 3; Fig. 5a,e). A peak at $Ex_{max}/Em_{max} = 240/445$ nm was consistently the most prominent one, and similar to peak A in Coble et al. (1998) indicating humic material (Fellman et al. 2010). The second most dominant peak was at $Ex_{max}/Em_{max} = 310/410$ nm, similar to the marine UVA humic-like peak M reported in previous studies and associated both with biological activity as well as terrestrial and anthropogenic sources (Fellman et al. 2010). A third peak at $Ex_{max}/Em_{max} = 280/(310–330)$ nm has fluorescence

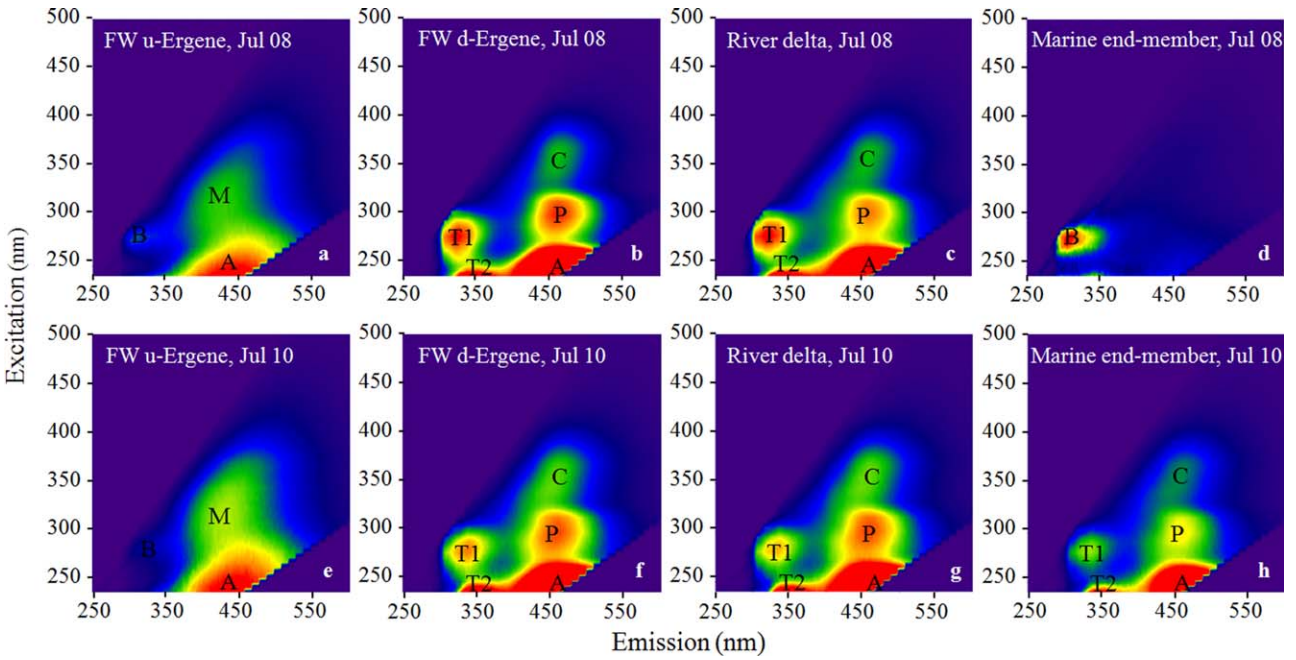

Fig. 5. CDOM fluorescence EEMs along the Evros river under (a–d) dry conditions in July 2008, and (e–h) under wet conditions in July 2010. Gradients are shown upstream and downstream of the confluence with Ergene (u- and d-Ergene, respectively), in the main Evros delta and at the marine end-member off the main delta (S12–S13). Fluorescence is shown in relative units.

characteristics similar to the protein-like peak B (tyrosine), which previous studies suggested to be indicative of biological activity, microbial processing, and relatively degraded peptide material (Yamashita and Tanoue 2004).

Freshwater CDOM directly downstream of the merging with Ergene showed a distinctive fluorescence footprint (Table 3; Fig. 5b,f). Peak A increased on average by a factor of 9, was still the most prominent one, and was slightly red-shifted. Peak M was absent. The protein-like peak increased, on average, by a factor of 11 and was at $Ex_{max}/Em_{max} = 280/335$ nm, resembling tryptophan fluorescence (T1) and indicative of intact proteins or less degraded peptide material (Fellman et al. 2010). Three additional peaks were identified. A peak at $Ex_{max}/Em_{max} = 240/350$ nm, similar to the short UV excitation component of tryptophan-like fluorescence (T2), was the second most pronounced peak after A (Hudson et al. 2008). A peak at $Ex_{max}/Em_{max} = 360/460$ nm, is similar to the UVC humic-like peak C in Coble et al. (1998). A very well defined peak at $Ex_{max}/Em_{max} = 300/460$ nm was prominent in all (and only those) CDOM samples affected by the Ergene outflow. This peak is not common in the literature, and will be referred to here as peak P. Variability in P : A and C : A was strongly correlated with discharge from Ergene D_{ERG} ($r = 0.91$, $n = 7$, $p = 0.004$, and $r = 0.90$, $n = 7$, $p = 0.005$, respectively). Both ratios remained unchanged during transport to the coastal zone (Table 3). With the exception of October 2008 when the dam was operating, this five-peak CDOM fluorescence signature persisted along the full extent of the Evros main stem, from S4 down to the river mouth, with a very consistent relative contribution among different fluorescence components (Figs. 5c,g, 6c; Table 3). It was also observed in the Aegean coastal waters under freshwater influence, as in July 2010, although peaks T1 and T2 were more pronounced relative to peak A in the coastal environment (Fig. 5h; Table 3). Under low freshwater influence (July 2008, October 2008), this five-peak fluorescence footprint was not detected at the marine end-member. Instead, coastal CDOM was characterized by a fluorescence signal with dominant contribution by the protein-like fluorescence component, a small contribution from peak A, and occasionally small contributions from the short UV excitation component of protein-like fluorescence (Fig. 5d; Table 3).

In October 2008, CDOM in the Evros brackish marshes had a fluorescence signal that was different than that of CDOM from other sources in Evros (freshwater or marine). It was very similar to that of CDOM exported from brackish tidal marshes (primarily vegetated by *Spartina patens, Scirpus olneyi*, and *Phragmites australis*; Tzortziou et al. 2008) in the Chesapeake Bay estuary, along the Eastern coast of the United States (Fig. 7). Peaks A, C, and B were present in CDOM from both marsh environments, at very similar relative contributions (Table 3). CDOM collected from the river mouth (S9–S10) in October 2008 was characterized by the same three peaks, suggesting marsh influence (Fig. 6c). During this river flow regime, the five-peak CDOM fluorescence footprint identified at the merging with Ergene was observed

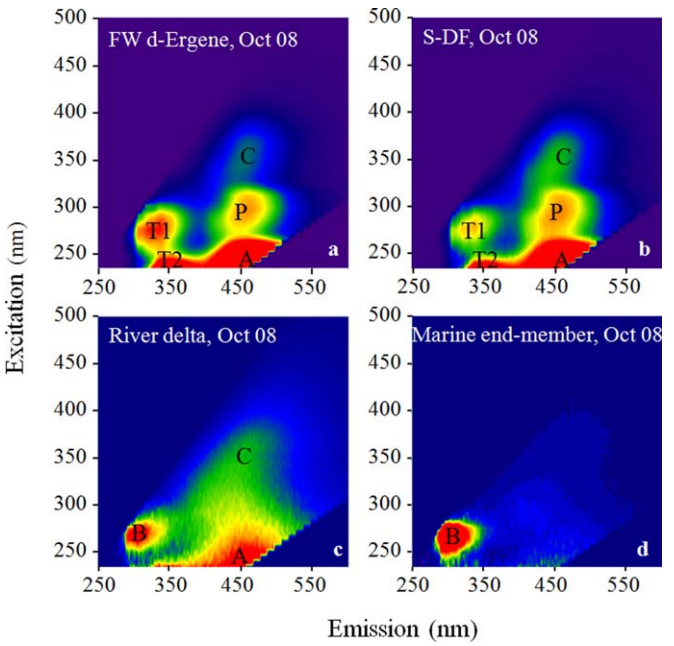

Fig. 6. Fluorescence EEMs measured on CDOM collected in October 2008 from (a) Evros downstream of the confluence with Ergene (FW d-Ergene), (b) the coastal water receiving the diverted river flow (S-DF), (c) downstream of the dam in the river delta off the Evros main stem, and (d) the marine end-member off the Evros main stem.

only in the coastal waters off the Turkish channel receiving the redirected freshwater discharge (S-DF, Fig. 6a,b).

DOM molecular weight distribution

DOM upstream of S3 showed five peaks in our measured SEC elution curves, at elution times 19.7 min (with a shoulder at 19.1 min), 20.5 min, 21.9 min, 24.1 min, and 24.8 min (Fig. 8a). Downstream of the merging with Ergene (S4), DOM showed an additional elution peak at 23.6 min, a considerable increase in the larger MW fraction components (left shoulder of first peak), and changes in the relative contributions of the two peaks at longer retention times, which correspond to smaller MW fraction components. Almost identical MW distribution was found for CDOM at S-DF, with a small decrease in the relative contribution of the larger and smaller MW DOM components. Both M_w and polydispersity increased downstream the Ergene influence. M_w increased from 970 at S3 to 1166 at S4, and remained relatively high (1018) in the coastal waters receiving the freshwater outflow (S-DF). Polydispersity increased from 2.32 at S3 to 2.91 at S4 and 2.55 at S-DF.

DOM collected from the Evros marshes (salinity 29.7) showed three distinct elution peaks that were very similar to the peaks measured on CDOM exported from the Chesapeake Bay brackish marshes during the fall of 2008 (measurements at low tide, salinity 14.3) (Fig. 8).

Discussion

Dissolved organic carbon dynamics

In a review study of the environmental state of 15 river basins that cover 83% of the Balkan river flow to the Mediterranean and largely encompass the physicogeographical diversity of the Balkan Peninsula, the Evros was among the most polluted (Skoulikidis 2009). It was also the only one characterized by "bad quality" status for all measured nutrients. Industrial and urban activities in the three countries sharing this basin, combined with a high proportion of agricultural land and forests, are expected to result in organic matter enrichment (Abril et al. 2002). Indeed, DOC concentrations in the Evros have been reported to be the highest among 13 major rivers that collectively contribute > 75% of the total Greek peninsula runoff to the Mediterranean (Skoulikidis 2009). Among these, transboundary rivers were the most polluted with the Evros at the top, followed by the Axios/Vardar river shared between Greece and the Former Yugoslav Republic of Macedonia (Skoulikidis 2002).

Our measurements were consistent with previous studies in the Evros that reported [DOC] in the range 2.09–3.87 mg

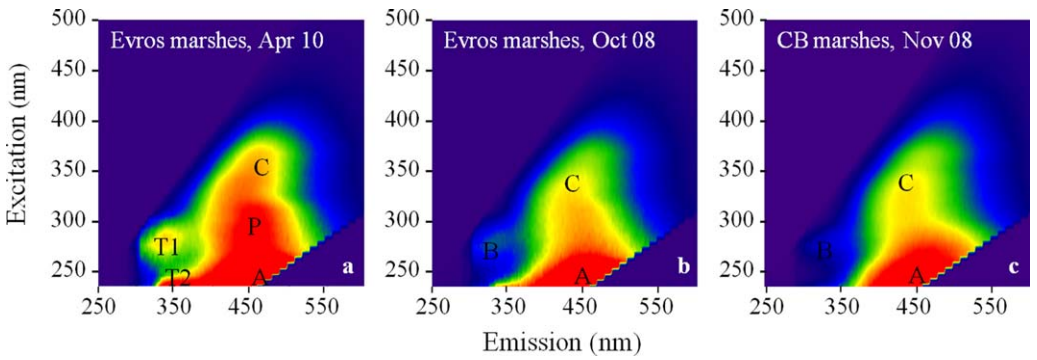

Fig. 7. CDOM fluorescence EEMs in the Evros coastal marshes (a) in April 2010 when the dam was not operating and (b) in October 2010 when the dam was operating and the marshes were not influenced by freshwater outflow (mid panel). (c) The fluorescence EEM measured on CDOM collected from the Chesapeake Bay (CB) brackish marshes in November 2008.

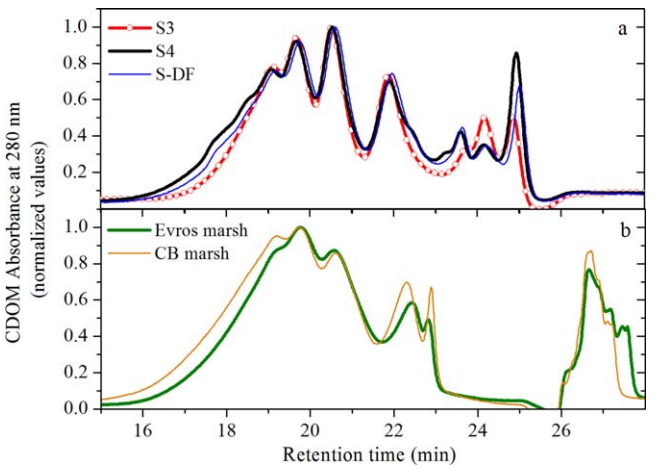

Fig. 8. Elution curves of DOM collected during our sampling in October (dam operational). (a) Results for DOM collected from sites S3 (upstream of the merging with Ergene), S4 (downstream of the merging with Ergene), and S-DF (coastal site affected by the redirected freshwater flow). Salinity at all sites was zero. (b) Elution curves of DOM collected from the Evros marshes (salinity = 29.7) and the brackish Chesapeake Bay marshes (salinity = 15). Results were normalized to maximum measured values. Peaks at smaller elution times correspond to larger molecular size DOM.

L^{-1} and an average of 2.77 mg L^{-1} (Skoulikidis 2009). However, our results also revealed that [DOC] can reach considerably higher levels, associated with marsh export of carbon-rich material nonpoint pollution sources and (Table 2). Compared to other major southern European coastal catchments, such as Po, Rhone and Arno (Table 4), [DOC] in the Evros delta and coastal waters reached higher values, similar to those reported for higher latitude, turbid, and highly polluted European estuaries (Abril et al. 2002; Mattsson et al. 2009).

A large fraction of DOC in Evros (40–80%) was colored. Our estimates of nonabsorbing DOC are lower compared to values reported for the Baltic Sea and the Rhine river plume (Ferrari et al. 1996; Ferrari 2000; Kowalczuk et al. 2010), but agree with data reported for eutrophic estuarine and coastal waters in the Tyrrhenian Sea, Chesapeake Bay, and Delaware Bay mouth, as well as freshwater systems in the North America and United Kingdom, where nonabsorbing DOC was in the range 0.6-1.2 mg L^{-1} (Seritti et al. 1998; Del Vecchio and Blough 2004; Carter et al. 2012). They also agree with previous studies showing that absorbing DOC can contribute as much as 70-80% to the total DOC pool in nearshore regions where river inputs are dominant (Oliveira et al. 2006). Among the non- or weakly-absorbing DOC substances, carbohydrates and urea typically represent the main fraction (Ferrari et al. 1996). During our sampling, the average contribution of total carbohydrates to DOC in Evros was in the range 20–30% (Pitta et al. 2014), in agreement with our optical analyses. Similarly, in the case of the Taylor River in the Florida Everglades, the nonabsorbing fraction, such as carbohydrates, represented only 35% of the DOC compared with the coastal bay the river discharges into, where carbohydrates represented 77% of DOC (Maie et al. 2005) due to a shift in DOC sources from soils and terrestrial higher plants to seagrass communities. In addition to such biologically controlled nonabsorbing DOC inputs, it has also been reported that the nonabsorbing fraction of DOC can be driven by storm-induced hydrological events in rain-forest streams (Pereira et al. 2014). Considering that such influences were relatively short-lived in tropical rainforest streams (ca. nine hours; Pereira et al. 2014), they may be less important in more arid regions, such as the one under study here.

Influence of anthropogenic pressures on DOM quality

Changes in the CDOM optical signature indicated strong variability in the source, composition, and distribution of DOM, associated both with natural processes and anthropogenic pressures. The observed range in S_{CDOM} and a^*_{CDOM} in the upper river, and the dominant role of peak A in fluorescence EEMs, reveal a major contribution of high MW, highly aromatic, humic DOM (Stewart and Wetzel 1980; Chin et al. 1994; Coble et al. 1998). Similar S_{CDOM} and a^*_{CDOM} values were reported by Seritti et al. (1998) for the Arno river ($S = 0.0167$ nm^{-1}, $a^*_{CDOM}(355) = 1.17$ m^{-1}) where, similarly to Evros, DOM has a mixed allochthonous (industrial, agricultural, urban) origin (Dinelli et al. 2005). The large contribution by peak M, associated with biological activity but also found often in agricultural catchment runoff (Fellman et al. 2010), and the good correlation between BIX and Chl *a* suggest some recent autochthonous DOM component from biological activity, but combined with the observed range in BIX (< 1.0) further indicate an important humic character (Huguet et al. 2009) possibly associated with agricultural run-off. This is consistent with previous studies reporting that agricultural activities are among the most important sources of pollutants along the Bulgaria-Greece border of the Evros watershed (Nikolaou et al. 2008). Agricultural land and forests are the main land uses in this section of the river (Dimitriou et al. unpubl.). Strong contributions of highly absorbing lignin and polyphenol aromatic humic compounds from the soil, forested watershed, and litterfall decomposition would, thus, be expected. Indeed, peak B, a good indicator of low MW terrestrial polyphenolic structures especially in environments with high contributions of humic substances (Seritti et al. 1998; Scully et al. 2004), was the third major peak identified in the CDOM fluorescence EEMs. The noncorrelation between Chl *a* and DOC suggests that the higher DOC amounts observed during the warm summer months in the upper river (particularly following high precipitation conditions in July 2010) were not driven by biological activity. Rather, the observed seasonal variability in DOC could be related to higher soil organic carbon concentrations during the growing season of terrestrial vegetation,

and the greater soil temperature, leaching efficiency, and flushing out of DOC from the surrounding forest organic horizons during summer (Gueguen et al. 2006). The observed high correlation between the degree of humification of DOM and total precipitation in this section of the river indicates an increased contribution of strongly humic terrestrial DOM under increased catchment runoff, consistent with Oliveira et al. (2006).

The dramatic shift in CDOM optical signature directly downstream of the merging with Ergene, combined with the more than an order of magnitude increase in NH_4^+, the > 2-fold increase in Cl^-, and the twofold increase in DOC, highlighted the importance of the Ergene river as a major source of allocthonous inputs of carbon, nutrients, and pollutants in this system. This is consistent with Sakcali et al. (2009), who compared water quality in the three major tributaries flowing into Ervos: the Ergene, the Tunca, and the Arda river (the last two merging with Evros upstream of our northernmost sampling site) and found particularly high pollution levels in the Ergene river. Water samples from Ergene had the highest sulfate and nitrogen concentrations, the lowest DO levels, and considerably higher biological (BOD) and chemical oxygen demand (COD) values (by more than a factor of 5) (Sakcali et al. 2009).

With 11,325 km^2 of drainage area, Ergene is one of the biggest river basins in the Turkish Thrace Region and a typical example of severe environmental deterioration due to rapid urbanization and industrialization (Güneş and Talinli 2013). Both urban wastewater and solid waste inputs in the river have increased the past decades (UNECE 2011). A total of about 1500 industries in the region flush their effluents directly into the main stem of the river and its tributaries, and it is estimated that 80-85% of the total flow in Ergene is from wastewater (Güneş and Talinli 2013). Leather tannery wastewater, municipal effluents, and uncontrolled landfill leachates contribute to pollution (Güneş et al. 2008; Özkan et al. 2010). A recent ecological assessment of the Ergene river waters and sediments reported severe toxicity to *Vibrio fisheri* (Güneş et al. 2008). Chloride and ammonium are good indicators of anthropogenic sources, including inputs of municipal waste leachates, farm drainage, piggery wastes, sewage effluent, and agricultural run-off from the use of nitrogenous fertilizers (Panno et al. 2005). Previous measurements at several locations along the Ergene river showed particularly high levels of chloride and ammonia, with average Cl^{-1} and NH_3 levels of 378 mg L^{-1} and 0.95 mg L^{-1}, respectively, at the station closest to the confluence with Evros (Table 2 in Özkan et al. 2010). High values of ammonium concentrations (1.9–12 mg L^{-1}) were reported by Güneş et al. (2008), who classified water quality as category IV (i.e., too polluted and should be used after treatment processes only for industrial purposes). These results agree with the increase in NH_4^+ and Cl^{-1} we consistently measured downstream the merging of Evros with Ergene. Although detailed measurements of water optical properties in Ergene are not available in the literature, Güneş et al. (2008) reported high values of organics and color (only absorbance at 340 nm was measured), particularly near the most urbanized and industrialized areas of Çorlu and Çerkezköy.

Our findings of an increase in a^*_{CDOM}, decrease in S_{CDOM}, increase in peak A by almost an order of magnitude, and the presence of a well defined peak C downstream of the merging with Ergene, indicate an increased input of strongly colored, high MW, humic DOM, such as diagenetic products of tannins or lignin-derived organic matter (Maie et al. 2007). An even larger increase, however, was observed in the protein-like fluorescence peak, which transitioned from tyrosine-like B to tryptophan-like T. Such a large contribution from peak-T (both T1 and T2 components) is characteristic of areas influenced by sewage (both treated and untreated), because sewage-derived DOM is dominated by organic matter originating from microbial activity (Baker 2002; Hudson et al. 2008). Interestingly, downstream of the merging with Ergene, the BIX index became inversely correlated with Chl *a* and positively correlated with discharge at Yenicegörece, further suggesting input of DOM of bacterial origin. Consistent with these results, the observed SEC traces showed a shift to an enhanced high-MW DOM in the upper MW range (16-18 min in Fig. 8a) and an absolute increase in the average-weight MW from S3 to S4, due to enhancement of humic-like materials. At the same time the low MW range for S4 was also enhanced compared to S3 (23 min and 25 min in Fig. 8a), possibly due to DOM components associated with sewage, peptide material or dissolved amino-acids.

Under heavy precipitation conditions, the distinctive five-peak CDOM fluorescence footprint of input from Ergene persisted across the full extent of the Evros river and into the coastal zone. Among these five fluorescence components, the relatively unknown, but in our case very well-defined, round-shaped peak P was observed on all (and only those) samples influenced by the Ergene outflow. The spectral location and shape of peak P are similar to the fluorescence properties of DOM associated with leaching of optical brighteners or fluorescent whitening agents (Baker 2002). Textile industries using toxic dyes and bleaching processes, are indeed among the main sources of pollution in the Ergene (Güneş et al. 2008; Özkan et al. 2010). Fluorescence peaks in a similar spectral region were reported previously by Saadi et al. (2006) and Butturini and Ejarque (2013) for relatively biorefractory humic DOM in rivers influenced by anthropogenic pollution. We found that peak P was absent in the freshwater DOM upstream the merging with Ergene, and was not detected in any of the samples collected from the estuarine or coastal waters off the Evros main stem when the dam diverted the river flow in October 2008. Yet, peak P clearly tracked the influence of the redirected freshwater plume on the Turkish coastal waters. The direct association of peak P with Ergene inputs and the strong correlation between the

ratio P : A and discharge at Yenicegörece suggest that continuous monitoring of peak P could provide a powerful tool, a rapid and sensitive proxy for detecting and assessing the origin, transport, and spatial extent of this allochthonous DOM input in the Evros system.

Effects of dam operation on downstream DOM dynamics

The construction of dams has become one of the most controversial issues in global efforts to strengthen regional economies, while at the same time balancing the environmental and socioeconomic benefits of healthy ecosystems (Richter and Thomas 2007). Regulation of dam operations becomes particularly challenging in shared rivers, where the benefits and risks of dams are quite different for different countries along the river's course. Although in this study we were not able to examine the influence of large reservoirs, we were able to capture some of the influences that smaller dams have on downstream water quality, salinity regimes, and biogeochemical properties. Operation of the dam downstream of S7 resulted in statistically significantly different nearshore optical, physicochemical, and biochemical properties. The immediate effect of the dam extended from the Evros marshes to the Aegean coastal zone and was, mainly, twofold. First, the redirection of the flow of upstream nutrients, carbon, and pollutants, and, second, the reduction in freshwater discharge and saltwater intrusion into the marsh and almost eight kilometers into the river.

Tidal marshes have been identified as consistent sources of optically distinctive, aromatic-rich, humic and highly colored DOM to adjacent estuaries (Tzortziou et al. 2008). Anthropogenic contributions of DOM in some estuaries with extensive wetlands are often masked by wetland-exported DOM, despite extensive urbanization and agricultural land use (Fellman et al. 2011). We found the opposite in the Evros estuary, where the influence of marshes on DOM quality was typically masked by upstream anthropogenic inputs (Figs. 3–5). In the absence of freshwater river runoff, however, (i.e., when the dam was operational) the brackish Evros marshes were the main source of DOC-rich, highly aromatic, and humic DOM to the delta (Tables 2–3). Under such conditions, DOM in the Evros marshes and adjacent delta had an optical footprint and a molecular-weight distribution signature that were almost identical to that of DOM derived from other brackish tidal marshes having similar vegetation characteristics but located in a very different environment, such as the eutrophic Chesapeake Bay (Figs. 7, 8; Table 3). The dam operation blocked the majority of upstream anthropogenic inputs. Still, the influence of the Ergene inputs was clear in the DOM fluorescence signal and MW distribution measured in the Turkish coastal waters receiving the diverted river flow, highlighting the predominance and refractory character of the DOM associated with this anthropogenic source.

River flow alteration by the dam reduced DOC concentrations in the Greek part of the Evros delta to almost half and lowered $a_{CDOM}(300)$ to one third (Table 2), improving downstream water clarity. At the same time, however, the dam operation resulted in changes in salinity and availability of inorganic nutrients in coastal waters (Tables 1–2; Fig. 2). The optical signature of CDOM in the Evros delta when the dam was operating clearly indicates DOM of marine origin with low degree of humification, consistent with the observed intrusion of saltwater > 8 km into the river. At the interface between the land and the ocean, the Evros marshes are naturally subject to considerable variability in salinity regimes. During our measurements covering both ebbing and flooding tides during both wet and dry seasons, salinity in the Evros delta ranged from 0 to 14 when the dam was not operating. Intrusion of saltwater when the dam was operating caused an abrupt increase in salinity, reaching almost 30 in the marshes. Such changes in salinity regimes may directly or indirectly influence biogeochemical cycles, carbon mineralization and greenhouse gas production in coastal wetland ecosystems (Neubauer et al. 2013).

Conclusions

Our findings have important implications for environmental monitoring and assessment in the Evros and other vulnerable transboundary rivers and wetland ecosystems, particularly in light of accelerated climate change and continued human pressures. Our measurements of CDOM optical signature and the direct association of peak P with DOM input from the severely polluted Ergene allowed to: (1) identify, track, and assess the spatial extent and distribution of this allocthonous DOM input under different hydrologic conditions (high vs. low runoff) and anthropogenic disturbances (dam operational or not), and (2) examine influences on carbon quality in downstream freshwater, wetland, and marine ecosystems. These results could have direct applications to programs focusing on pollution detection and monitoring in shared rivers where management of water quality remains largely ineffective. Most of the present climate models in the Eastern Mediterranean area indicate higher temperatures, increased frequency and intensity of drought, and increased vulnerability to flooding due to intensification of heavy precipitation events (Christensen et al. 2013). Water resources will be stressed in Southern Europe, North Africa, and the Near East where water availability is already low, making effective management of these limited resources even more challenging. Dams may play an increasingly important role in protecting water resources and regulating human exposure to natural hazards (Brown et al. 2009), at the same time changing salinity regimes, redirecting upstream anthropogenic pollution, and affecting carbon quality in downstream ecosystems, as this study showed. Coordinated monitoring of specific CDOM optical properties

(such as fluorescence peak P) and other sensitive water quality and biogeochemical state indicators are critically needed to better understand the influence of current (and future) natural and anthropogenic pressures on biogeochemical cycles and ecosystem dynamics in transboundary rivers and their coastal wetlands.

References

Abboudi, M., and others. 2008. Effects of photochemical transformations of dissolved organic matter on bacterial metabolism and diversity in three contrasting coastal sites in the northwestern Mediterranean Sea during summer. Microb. Ecol. **55**: 344–357. doi:10.1007/s00248-007-9280-8

Abril, G., M. Nogueira, H. Etcheber, G. Cabecadas, E. Lemaire, and M. J. Brogueira. 2002. Behaviour of organic carbon in nine contrasting European estuaries. Estuar. Coast. Shelf Sci. **54**: 241–262. doi:10.1006/ecss.2001.0844

Angelidis, P., M. Kotsikas, and N. Kotsovinos. 2010. Management of upstream dams and flood protection of the transboundary river Evros/Maritza. Water Resour. Manage. **24**: 2467–2484. doi:10.1007/s11269-009-9563-6

Arar, E. J., and G. B. Collins. 1997. Method 445.0, *in vitro* determination of chlorophyll *a* and pheophytin *a* in marine and freshwater algae by fluorescence. In: Methods for the determination of chemical substances in marine and estuarine environmental matrices, EPA/600/R-97/072, 2nd edn. National Exposure Research Laboratory, Office of Research and Development, USEPA, Cincinnati, OH, 1–22.

Babin, M., D. Stramski, G. M. Ferrari, H. Claustre, A. Bricaud, G. Obolensky, and N. Hoepffner. 2003. Variations in the light absorption coefficients of phytoplankton, non algal particles, and dissolved matter in coastal waters around Europe. J. Geophys. Res. **108**: 3211. doi:10.1029/2001JC000882

Baker, A. 2002. Fluorescence excitation-emission matrix characterization of river waters impacted by a tissue mill effluent. Environ. Sci. Technol. **36**: 1377–1382. doi:10.1021/es0101328

Berto, D., M. Giani, F. Savelli, E. Centanni, C. R. Ferrari, and B. Pavoni. 2010. Winter to spring variations of chromophoric dissolved organic matter in a temperate estuary (Po River, northern Adriatic Sea). Mar. Environ. Res. **70**: 73–81. doi:10.1016/j.marenvres.2010.03.005

Bricaud, A., A. Morel, and L. Prieur. 1981. Absorption by dissolved organic matter of the sea (yellow substance) in the UV and visible domains. Limnol. Oceanogr. **26**: 43–53. doi:10.4319/lo.1981.26.1.0043

Brown, P. H., D. Tullos, B. Tilt, D. Magee, and A. T. Wolf. 2009. Modeling the costs and benefits of dam construction from a multidisciplinary perspective. J. Environ. Manage. **90**: 303–311. doi:10.1016/j.jenvman.2008.07.025

Butturini, A., and E. Ejarque. 2013. Technical Note: Dissolved organic matter fluorescence—a finite mixture approach to deconvolve excitation-emission matrices. Biogeosciences **10**: 5875–5887. doi:10.5194/bg-10-5875-2013

Carter, H. T., E. Tipping, J. F. Koprivnjak, M. P. Miller, B. Cookson, and J. Hamilton-Taylor. 2012. Freshwater DOM quantity and quality from a two-component model of UV absorbance. Water Res. **46**: 4532–4542. doi:10.1016/j.watres.2012.05.021

Cauwet, G. 1994. HTCO method for dissolved organic carbon analysis in seawater: Influence of catalyst on blank estimation. Mar. Chem. **47**: 55–64. doi:10.1016/0304-4203(94)90013-2

Chin, Y. P., G. Aiken, and E. Oloughlin. 1994. Molecular-weight, polydispersity, and spectroscopic properties of aquatic humic substances. Environ. Sci. Technol. **28**: 1853–1858. doi:10.1021/es00060a015

Christensen, J. H., and others. 2013. Climate phenomena and their relevance for future regional climate change. In T. F. Stocker, D. Qin, G.-K. Plattner, M. Tignor, S. K. Allen, J. Boschung, A. Nauels, Y. Xia, V. Bex and P. M. Midgley [eds.], Climate change 2013: The physical science basis. Contribution of Working Group I to the IPCC Fifth Assessment Report of the Intergovernmental Panel on Climate Change. Cambridge Univ. Press.

Coble, P. G., C. E. Del Castillo, and B. Avril. 1998. Distribution and optical properties of CDOM in the Arabian Sea during the 1995 SW monsoon. Deep-Sea Res. II **45**: 2195–2223. doi:10.5670/oceanog. 2004.47

De Groot, R. S., M. A. A. Stuip, C. M. Finlayson, and N. Davidson. 2006. Valuing wetlands: Guidance for valuing the benefits derived from wetland ecosystem services, Ramsar Technical Report No. 3/CBD Technical Series No. 27. Ramsar Convention Secretariat, Gland, Switzerland & Secretariat of the Convention on Biological Diversity, Montreal, Canada.

Del Vecchio, R., and N. V. Blough. 2004. Spatial and seasonal distribution of chromophoric dissolved organic matter and dissolved organic carbon in the Middle Atlantic Bight. Mar. Chem. **89**: 169–187. doi:10.1016/j.marchem.2004.02.027

Dinelli, E., G. Cortecci, F. Lucchini, and E. Zantedeschi. 2005. Sources of major and trace elements in the stream sediments of the Arno river catchment (northern Tuscany, Italy). Geochem. J. **39**: 531–545. doi:10.2343/geochemj.39.531

Fellman, J. B., E. Hood, and R. G. M. Spencer. 2010. Fluorescence spectroscopy opens new windows into dissolved organic matter dynamics in freshwater ecosystems: A review. Limnol. Oceanogr. **55**: 2452–2462. doi:10.4319/lo.2010.55.6.2452

Fellman, J. B., K. Petrone, and P. F. Grierson. 2011. Source, biogeochemical cycling, and fluorescence characteristics of dissolved organic matter in an agro-urban estuary. Limnol. Oceanogr. **56**: 243–256. doi:10.4319/lo.2011.56.1.0243

Ferrari, G. 2000. The relationship between chromophoric dissolved organic matter and dissolved organic carbon in the European Atlantic coastal area and in the West Mediterranean Sea (Gulf of Lions). Mar. Chem. **70**: 339–357. doi:10.1016/S0304-4203(00)00036-0

Ferrari, G., M. D. Dowell, S. Grossi, and C. Targa. 1996. Relationship between optical properties of chromophoric dissolved organic matter and total concentration of dissolved organic carbon in southern Baltic Sea region. Mar. Chem. **55**: 299–316. doi:10.1016/S0304-4203(96)00061-8

Giorgi, F. 2006. Climate change hot-spots. Geophys. Res. Lett. **33**: L08707. doi:10.1029/2006GL025734

Groombridge, B. 1999. Shared wetlands and river basins of the World: Preliminary findings of a GIS analysis. Ramsar COP7 DOC. 20.1 Report. World Conservation Monitoring Centre.

Guéguen, C., L. Guo, D. Wang, N. Tanaka, and C. C. Hung. 2006. Chemical characteristics and origin of dissolved organic matter in the Yukon River. Biogeochemistry **77**: 139–155.

Güneş, E., and I. Talinli. 2013. A site-specific index to control the total effect of point sources discharges and to achieve 'Good Chemical Status' in effluent dependent and effluent dominated water bodies: Application on Ergene River Basin. Water Resour. Manage. **27**: 221–237. doi:10.1007/s11269-012-0180-4

Günes, E. H., Y. Günes, and I. Talinli. 2008. Toxicity evaluation of industrial and land base sources in a river basin. Desalination **226**: 348–356. doi:10.1016/j.desal.2007.02.116

Hudson, N., A. Baker, D. Ward, D. M. Reynolds, C. Brunsdon, C. Carliell-Marquet, and S. Browning. 2008. Can fluorescence spectrometry be used as a surrogate for the Biochemical Oxygen Demand (BOD) test in water quality assessment? An example from South West England. Sci. Total Environ. **391**: 149–158. doi:10.1016/j.scitotenv.2007.10.054

Huguet, A., L. Vacher, S. Relexans, S. Saubusse, J. M. Froidefond, and E. Parlanti. 2009. Properties of fluorescent dissolved organic matter in the Gironde Estuary. Org. Geochem. **40**: 706–719. doi:10.1016/j.orggeochem.2009.03.002

Jaffé, R., and others. 2012. Dissolved organic matter in headwater streams: Compositional variability across climatic regions of North America. Geochim. Cosmochim. Acta **94**: 95–108. doi:10.1016/j.gca.2012.06.031

Kanellopoulos, T. D., M. O. Angelidis, D. Georgopoulos, and A. P. Karageorgis. 2009. Fate of the Evros River suspended particulate matter in the N Aegean Sea. Environ. Geol. **57**: 1729–1738. doi:10.1007/s00254-008-1454-2

Kowalczuk, P., M. Zabłocka, S. Sagan, and K. Kuliński. 2010. Fluorescence measured in situ as a proxy of CDOM absorption and DOC concentration in the Baltic Sea. Oceanologia **52**: 431–471. doi:10.5697/oc.52-3.431

Lelieveld, J., and others. 2012. Climate change and impacts in the Eastern Mediterranean and the Middle East. Clim. Change **114**: 667–687. doi:10.1007/s10584-012-0418-4

Maie, N., N. M. Scully, O. Pisani, and R. Jaffe. 2007. Composition of a protein-like fluorophore of dissolved organic matter in coastal wetland and estuarine ecosystems. Water Res. **41**: 563–570. doi:10.1016/j.watres.2006.11.006

Maie, N., C. Yang, T. Miyoshi, K. Parish, and R. Jaffe. 2005. Chemical characteristics of dissolved organic matter in an oligotrophic subtropical wetland/estuarine ecosystem. Limnol. Oceanogr. **50**: 23–35. doi:10.4319/lo.2005.50.1.0023

Mattsson, T., P. Kortelainen, A. Laubel, D. Evans, M. Pujo-Pay, A. Räike, and P. Conan. 2009. Export of dissolved organic matter in relation to land use along a European climatic gradient. Sci. Total Environ. **407**: 1967–1976. doi:10.1016/j.scitotenv.2008.11.014

McKnight, D. M., E. W. Boyer, P. K. Westerhoff, P. T. Doran, T. Kulbe, and D. T. Andersen. 2001. Spectrofluorometric characterization of dissolved organic matter for indication of precursor organic material and aromaticity. Limnol. Oceanogr. **46**: 38–48. doi:10.4319/lo.2001.46.1.0038

Neubauer, S. C., R. B. Franklin, and D. J. Berrier. 2013. Saltwater intrusion into tidal freshwater marshes alters the biogeochemical processing of organic carbon. Biogeosciences **10**: 8171–8183. doi:10.5194/bg-10-8171-2013

Nikolaou, A. D., S. Meric, D. F. Lekkas, V. Naddeo, V. Belgiorno, S. Groudev, and A. Tanik. 2008. Multi-parametric water quality monitoring approach according to the WFD application in Evros trans-boundary river basin: Priority pollutants. Desalination **226**: 306–320. doi:10.1016/j.desal.2007.02.113

Obernosterer, I., and G. J. Herndl. 2000. Differences in the optical and biological reactivity of the humic and nonhumic dissolved organic carbon component of two contrasting coastal marine environments. Limnol. Oceanogr. **45**: 1120–1129. doi:10.4319/lo.2000.45.5.1120

Oliveira, J. L., M. Boroski, J. C. R. Azevedo, and J. Nozaki. 2006. Spectroscopic investigation of humic substances in a tropical lake during a complete hydrological cycle. Acta Hydrochim. Hydrobiol. **34**: 608–617. doi:10.1002/aheh.200400659

Özkan, N., J. Moubayed-Breil, and B. Çamur-Elipek. 2010. Ecological analysis of chironomid larvae (Diptera, Chironomidae) in Ergene River Basin (Turkish Thrace). Turk. J. Fish. Aquat. Sci. **10**: 93–99. doi:10.4194/trjfas.2010.0114

Panno, S. V., K. C. Hackley, H.-H. Hwang, S. Greenberg, I. G. Krapac, S. Landsberger, and D. J. O'Kelly. 2005. Database for the characterization and identification of the sources of sodium and chloride in natural waters of Illinois. Illinois State Geological Survey Open File Series 2005-1. 15 p, Champaign, IL.

Para, J., P. G. Coble, B. Charriere, M. Tedetti, C. Fontana, and R. Sempere. 2010. Fluorescence and absorption

properties of chromophoric dissolved organic matter (CDOM) in coastal surface waters of the northwestern Mediterranean Sea, influence of the Rhone River. Biogeosciences **7**: 4083–4103. doi:10.5194/bg-7-4083-2010

Pereira, R., and others. 2014. Mobilization of optically invisible dissolved organic matter in response to rainstorm events in a tropical forest headwater river. Geophys. Res. Lett. **41**: 1202–1208. doi:10.1002/2013GL058658

Pitta, E., and others. 2014. Dissolved organic matter cycling in eastern Mediterranean rivers experiencing multiple pressures. The case of the trans-boundary Evros River. Mediterr. Mar. Sci. **15**: 398–415. doi:10.12681/mms.565

Richter, B. D., and G. A. Thomas. 2007. Restoring environmental flows by modifying dam operations. Ecol. Soc. **12**: 12. Available from http://www.ecologyandsociety.org/vol12/iss1/art12/

Saadi, I., M. Borisover, R. Armon, and Y. Laor. 2006. Monitoring of effluent DOM biodegradation using fluorescence, UV and DOC measurements. Chemosphere **63**: 530–539. doi:10.1016/j.chemosphere.2005.07.075

Sakcali, S. M., R. Yilmaz, S. Gucel, C. Yarci, and M.Ozturk. 2009. Water pollution studies in the rivers of the Edirne Region–Turkey. Aquat. Ecosyst. Health Manage. **12**: 313–319. doi:10.1080/14634980903133757

Schaeffer, B. A., K. G. Schaeffer, D. Keith, R. S. Lunetta, R. Conmy, and R. W. Gould. 2013. Barriers to adopting satellite remote sensing for water quality management. Int. J. Remote Sensing **34**: 7534–7544. doi:10.1080/01431161.2013.823524

Scully, N. M., N. Maie, S. K. Dailey, J. N. Boyer, R. D. Jones, and R. Jaffe. 2004. Early diagenesis of plant-derived dissolved organic matter along a wetland, mangrove, estuary ecotone. Limnol. Oceanogr. **49**: 1667–1678. doi:10.4319/lo.2004.49.5.1667

Seritti, A., D. Russo, L. Nannicini, and R. Del Vecchio. 1998. DOC, absorption and fluorescence properties of estuarine and coastal waters of the northern Tyrrhenian Sea. Chem. Speciation Bioavailability **10**: 95–105. doi:10.3184/095422998782775790

Skoulikidis, N. 2002. Typological and qualitative characteristics of Greek-interregional rivers. Mediterr. Mar. Sci. **3**: 79–88. doi:10.12681/mms.260

Skoulikidis, N. 2009. The environmental state of rivers in the Balkans—a review within the DPSIR framework. Sci. Total Environ. **407**: 2501–2516. doi:10.1016/j.scitotenv.2009.01.026

Stewart, A. J., and R. G. Wetzel. 1980. Fluorescence—absorbance ratios—a molecular-weight tracer of dissolved organic-matter. Limnol. Oceanogr. **25**: 559–564. doi:10.4319/lo.1980.25.3.0559

Sugimura, Y., and Y. Suzuki. 1988. A high-temperature catalytic oxidation method for the determination of non-volatile dissolved organic carbon in seawater by direct injection of a liquid sample. Mar. Chem. **24**: 105–131. doi:10.1016/0304-4203(88)90043-6

Tzortziou, M., P. J. Neale, C. L. Osburn, J. P. Megonigal, N. Maie, and R. Jaffe. 2008. Tidal marshes as a source of optically and chemically distinctive colored dissolved organic matter in the Chesapeake Bay. Limnol. Oceanogr. **53**: 148–159. doi:10.4319/lo.2008.53.1.0148

United Nations Economic Commission for Europe (UNECE). 2011. Second Assessment of Transboundary Rivers, Lakes and Groundwaters. Geneva: United Nations Publication. Available from http://www.unece.org/?id=26343.

Vázquez, E., S. Amalfitano, S. Fazi, and A. Butturini. 2011. Dissolved organic matter composition in a fragmented Mediterranean fluvial system under severe conditions. Biogeochemistry **102**: 59–72. doi:10.1007/s10533-010-9421-x

Vázquez, E., A. M. Romaní, F. Sabater, and A. Butturini. 2007. Effects of the dry-wet hydrological shift on dissolved organic carbon dynamics and fate across stream-riparian interface in a Mediterranean catchment. Ecosystems **10**: 239–251. doi:10.1007/s10021-007-9016-0

Vignudelli, S., C. Santinelli, E. Murru, L. Nannicini, and A. Seritti. 2004. Distributions of dissolved organic carbon (DOC) and chromophoric dissolved organic matter (CDOM) in coastal waters of the northern Tyrrhenian Sea (Italy). Estuar. Coast. Shelf Sci. **60**: 133–149. doi:10.1016/j.ecss.2003.11.023

Wolf, A. T., J. Natharius, J. Danielson, B. Ward, and J. Pender. 1999. International river basins of the world. Int. J. Water Resour. Dev. **15**: 387–427. doi:10.1080/07900629948682

Yamashita, Y., and E. Tanoue. 2004. Chemical characteristics of amino acid-containing dissolved organic matter in seawater. Org. Geochem. **35**: 679–692. doi:10.1016/j.orggeochem.2004.02.007

Acknowledgments

We thank E. Moussoulis and A. Konstantinopoulou for assistance in the field and laboratory. This work was supported by a European Union Marie Curie Excellence Grant (project PreWEC, Grant #: MEXT-CT-2006-038331), a Marie Curie International Reintegration Grant (project Eco-DOM, Grant #: FP7-MC-IRG-208841), a National Science Foundation Grant from the Division of Environmental Biology (DEB) - Ecosystem Science Cluster (Grant #: DEB-0742185), and the George Barley Endowment. This is Southeast Environmental Research Center contribution 716.

Received 3 April 2014
Accepted 8 March 2015
Amended 28 February 2015

Associate Editor: Anna Romaní